Journal of Semiconductors
JOS iopscience.iop.org/jos
www.jos.ac.cn

High-operating-temperature MWIR photodetector based on a InAs/GaSb superlattice grown by MOCVD

Xiujun Hao, Yan Teng, He Zhu, Jiafeng Liu, Hong Zhu, Yunlong Huai, Meng Li, Baile Chen, Yong Huang, and Hui Yang

Citation: X J Hao, Y Teng, H Zhu, J F Liu, H Zhu, Y L Huai, M Li, B L Chen, Y Huang, and H Yang, High-operating-temperature MWIR photodetector based on a InAs/GaSb superlattice grown by MOCVD[J]. *J. Semicond.*, 2022, 43(1).
View online: https://doi.org/10.1088/1674-4926/43/1/012303

Articles you may be interested in

Strain-induced the dark current characteristics in InAs/GaSb type-II superlattice for mid-wave detector
Journal of Semiconductors. 2020, 41(6), 062302 https://doi.org/10.1088/1674-4926/41/6/062302

Theoretical simulation of T2SLs InAs/GaSb cascade photodetector for HOT condition
Journal of Semiconductors. 2018, 39(9), 094004 https://doi.org/10.1088/1674-4926/39/9/094004

InAs-based interband cascade lasers at 4.0 μm operating at room temperature
Journal of Semiconductors. 2018, 39(11), 114003 https://doi.org/10.1088/1674-4926/39/11/114003

Analysis of the growth of GaN epitaxy on silicon
Journal of Semiconductors. 2018, 39(3), 033006 https://doi.org/10.1088/1674-4926/39/3/033006

High order DBR GaSb based single longitude mode diode lasers at 2 μm wavelength
Journal of Semiconductors. 2018, 39(10), 104007 https://doi.org/10.1088/1674-4926/39/10/104007

Study of the morphology evolution of AlN grown on nano-patterned sapphire substrate
Journal of Semiconductors. 2019, 40(12), 122803 https://doi.org/10.1088/1674-4926/40/12/122803

关注微信公众号，获得更多资讯信息

Journal of Semiconductors
(2022) 43, 012303
doi: 10.1088/1674-4926/43/1/012303

ARTICLES

High-operating-temperature MWIR photodetector based on a InAs/GaSb superlattice grown by MOCVD

Xiujun Hao[1, 2], Yan Teng[1], He Zhu[1], Jiafeng Liu[1], Hong Zhu[1], Yunlong Huai[1], Meng Li[1, 2], Baile Chen[3], Yong Huang[1, †], and Hui Yang[1, 2]

[1]Key Laboratory of Nanodevices and Applications, Suzhou Institute of Nano-Tech and Nano-Bionics, CAS, Suzhou 215123, China
[2]School of Physical Science and Technology, ShanghaiTech University, Shanghai 201210, China
[3]School of Information Science and Technology, ShanghaiTech University, Shanghai 201210, China

Abstract: We demonstrate a high-operating-temperature (HOT) mid-wavelength InAs/GaSb superlattice heterojunction infrared photodetector grown by metal–organic chemical vapor deposition. High crystalline quality and the near-zero lattice mismatch of a InAs/GaSb superlattice on an InAs substrate were evidenced by high-resolution X-ray diffraction. At a bias voltage of –0.1 V and an operating temperature of 200 K, the device exhibited a 50% cutoff wavelength of ~ 4.9 μm, a dark current density of 0.012 A/cm^2, and a peak specific detectivity of 2.3×10^9 cm·Hz$^{1/2}$ /W.

Key words: HOT; MWIR; InAs/GaSb superlattice; aluminum-free; MOCVD

Citation: X J Hao, Y Teng, H Zhu, J F Liu, H Zhu, Y L Huai, M Li, B L Chen, Y Huang, and H Yang, High-operating-temperature MWIR photodetector based on a InAs/GaSb superlattice grown by MOCVD[J]. *J. Semicond.*, 2022, 43(1), 012303. http://doi.org/10.1088/1674-4926/43/1/012303

1. Introduction

The emergence of high-operating-temperature (HOT) mid-wavelength infrared (MWIR) photodetectors would lead to a reduction in the size, weight, and cost of the detection system[1]. Although InSb material is the most widely used HOT MWIR photodetector, InSb-based detection technology is plagued by its narrow bandgap (0.235 eV at 77 K) and operating temperature (~105 K)[2, 3]. A HgCdTe-based infrared detector operating near room temperature has been demonstrated[4], but is still limited by defect levels and very expensive substrates. One of the most competitive material systems of developing HOT photodetectors is InAs/GaSb type II superlattice (SL) due to its numerous advantages such as good material uniformity and low Auger recombination rates[5–7]. To suppress the dark current, several strategies were used to achieve HOT detectors including barrier structures such as PπMN structure[8–10] and pBiBn structure[11]. These high-performance heterojunction designs are usually grown in abundance by molecular beam epitaxy (MBE)[8–11]. On the other hand, the metal–organic chemical vapor deposition (MOCVD), as an alternative epitaxy technique, presents key advantages for high volume and low-cost production.

In this letter, we report a HOT MWIR InAs/GaSb SL photodetector with a 50% cutoff wavelength of 4.9 μm at 200 K based on an Al-free PNn structure grown by MOCVD, which demonstrates promising results compared to MBE-grown devices.

Correspondence to: Y Huang, yhuang2014@sinano.ac.cn
Received 31 MAY 2021; Revised 19 JUNE 2021.
©2022 Chinese Institute of Electronics

2. Experiment

2.1. Device design

In the PNn structure design, the electron blocking layer (N layer) is sandwiched between the P contact layer and the n absorption region, which was previously adopted for long wavelength infrared (LWIR) detection[12, 13]. By properly choosing the doping level and thickness of the N layer, the depletion region stretches mostly into this high bandgap layer but not the n absorption region, which is used for the suppression of generation–recombination and tunneling dark current. This Al-free PNn structure design is composed of a 1 μm 9 monolayer InAs/8 monolayer GaSb (9 ML/8 ML) mid-wavelength superlattice (MWSL) absorber ($n \sim 2 \times 10^{16}$ cm^{-3}), a 110 nm 4 ML/8 ML short-wavelength superlattice (SWSL) barrier layer ($N \sim 5 \times 10^{16}$ cm^{-3}) and a 200 nm 4 ML/8 ML SWSL contact layer ($P \sim 1 \times 10^{18}$ cm^{-3}). The same GaSb layer thickness in both MWSL and SWSL could lead to their valence band edges lining up reasonably closely[14] and result in a large conduction band offset. The energy-band diagram of the PNn device at 77 K is displayed in Fig. 1(a). In this case, the N-SWSL layer is designed to act as an electron barrier for the n-MWSL layer. The schematic cross-section of the PNn detector is shown in Fig. 1(b).

2.2. Device fabrication

The PNn structure device was grown on an InAs (001) substrate by MOCVD. Trimethylindium (TMIn), triethylgallium (TEGa), trimethylantimony (TMSb), and arsine (AsH_3) were used as precursors. Details of the material growth conductions can be found elsewhere[15]. High-resolution X-ray diffraction (HR-XRD) was used to evaluate material quality. Chlorine-based inductively coupled plasma (ICP) dry etching and plasma-enhanced chemical vapor deposition (PECVD) were used to define device mesas and grow SiO_2 passivation layer,

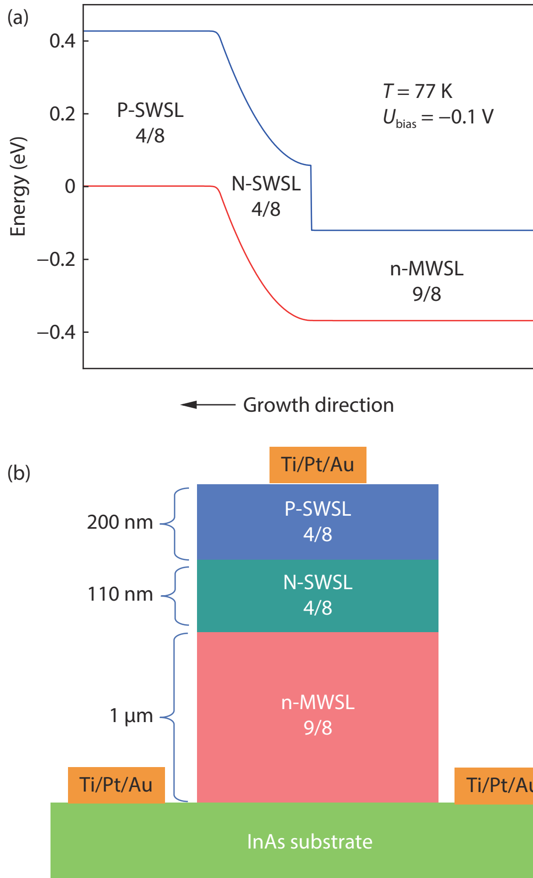

Fig. 1. (Color online) (a) Energy-band diagram of the PNn device at 77 K. (b) Cross-section of the PNn detector, where 4/8 and 9/8 stand for 4 monolayer InAs/8 monolayer GaSb and 9 monolayer InAs/8 monolayer GaSb, respectively.

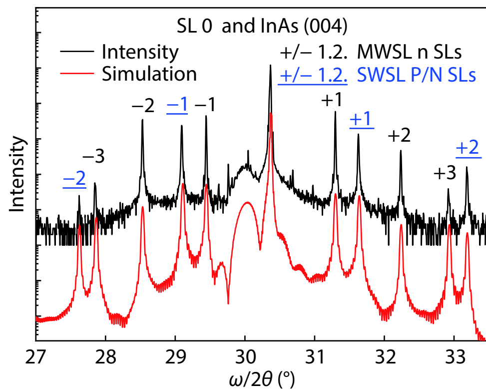

Fig. 2. (Color online) HR-XRD of the PNn structure device and the corresponding simulation curve.

respectively. Ti/Pt/Au metal stacks were deposited as device contact portions.

3. Results and discussions

Fig. 2 shows the HR-XRD data of the PNn device and the corresponding simulation curve. The periods of the MWSL and the SWSL are about 55.3 and 40.5 Å, respectively, which is in reasonable agreement with the device design. The angle separations between the 0-th peaks and the InAs substrate peak is only 3 and 53 arcsec for MWSL and SWSL, respectively, suggesting a well-balanced strain.

The dark current density (J_d) and the differential resistance-area product (RA) at different temperatures are given in Figs. 3(a) and 3(b). At −0.1 V, the PNn structure photodetector exhibits a J_d of 8.9 × 10^{-5} A/cm^2 at 150 K, whereas, at 200 K, J_d is 0.012 A/cm^2. The corresponding differential resistance-area products are 2832 and 48 Ω·cm^2 at 150 and 200 K, respectively. The electrical performance of this detector is comparable to those reported for the HOT MWIR SL detectors grown by MBE[10, 16]. Fig. 4 presents J_d as a function of detector temperature (ranging from 78 to 200 K) at a bias voltage of −0.1 V. The activation energies (ΔE) were fitted using J_{diff} ~ $T^3\exp[-E_a/(K_bT)]$[17]. The activation energy of about 253 meV was deduced at temperatures T > 135 K. This value is closed to the designed absorber bandgap, indicating that this HOT

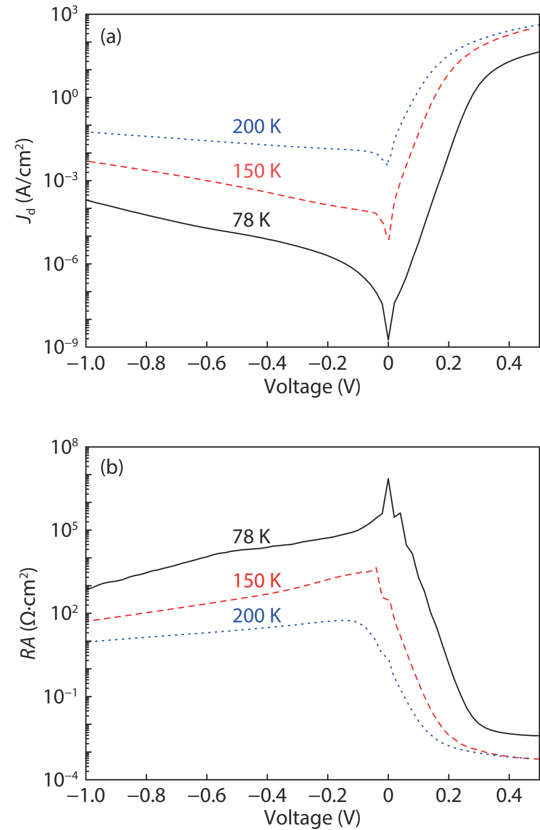

Fig. 3. (Color online) (a) J_d versus voltage at different temperatures. (b) RA versus voltage at different temperatures.

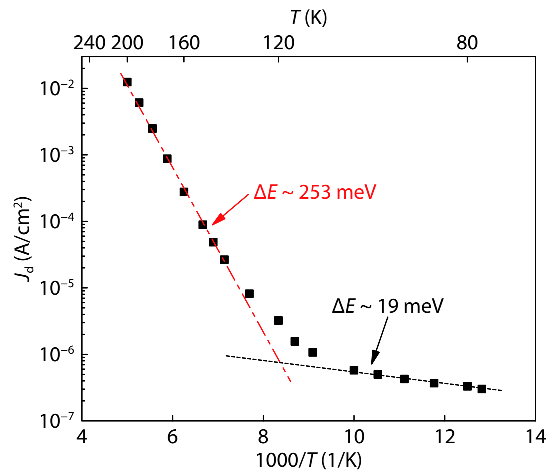

Fig. 4. (Color online) J_d as a function of temperature at a bias voltage of −0.1 V.

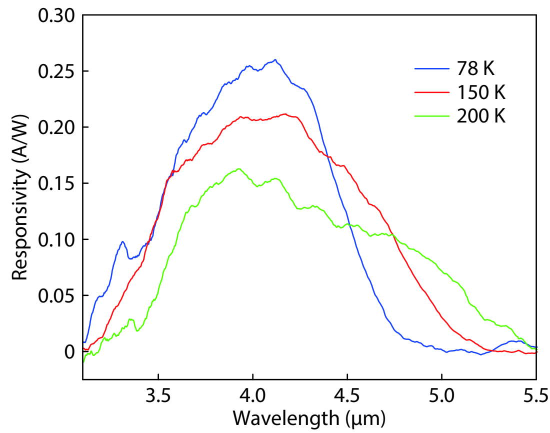

Fig. 5. (Color online) Spectral responsivity (R_λ) of PNn device at different temperatures.

Table 1. 50% cutoff wavelengths at 78, 150, and 200 K.

Temperature (K)	78	150	200
$\lambda_{50\% \text{ cutoff}}$ (μm)	4.5	4.7	4.9

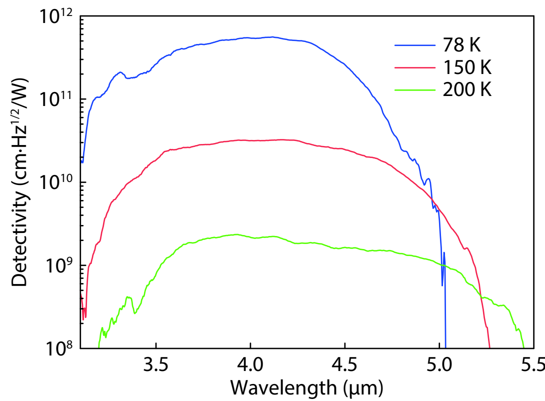

Fig. 6. (Color online) Specific detectivity (D^*) of the PNn device at different temperatures.

MWIR photodetector is dominated by the diffusion mechanism. However, as $T < 100$ K, activation energy is fitted to be as low as 19 meV, implying that tunneling or surface leakage current is a dominated mechanism in the PNn device.

Fig. 5 shows spectral responsivity (R_λ) of the PNn device at different temperatures, which was measured by FTIR system (Nicolet IS50) with a 1000 K blackbody source. It can be seen that the cutoff wavelength keeps increasing as the temperature increase. Table 1 shows the 50% cutoff wavelengths at 78, 150, and 200 K. Under 78 K and –0.1 V, the peak responsivity (R_λ) of 0.26 A/W was measured at 4.1 μm, corresponding to a quantum efficiency (QE) of 7.9%. The low QE is possibly due to the thinner absorption layer or/and a potential barrier between the N-SWSL layer and the n-MWSL layer.

The specific detectivity (D^*) at –0.1 V was estimated using the following equation:

$$D^* = R_\lambda \left(2qJ_\text{d} + \frac{4kT}{R_\text{d}A_\text{d}}\right)^{-\frac{1}{2}}, \tag{1}$$

where R_λ is the responsivity, q is the electronic charge, k and T is Boltzmann's constant and the temperature of the device, respectively. Fig. 6 shows specific detectivity (D^*) of the PNn device at different temperatures. At 78, 150, and 200 K, the D^* was calculated to be 5.6 × 10^{11}, 3.2 × 10^{10}, and 2.3 × 10^9 cm·Hz$^{1/2}$/W, respectively. The D^* decreases fast with temperature because of the exponentially increased dark current and reduced quantum efficiency. Although the D^* of the PNn structure is less than those of the state-of-the-art HOT MWIR detectors grown by MBE[10, 11], the PNn device structure grown by MOCVD shows potentials for HOT MWIR photodetectors.

4. Conclusions

In summary, an aluminum-free heterojunction PNn-structure InAs/GaSb superlattice HOT MWIR photodetector grown by MOCVD has been demonstrated with an operating temperature up to 200 K. At 200 K and –0.1 V, the device exhibited a J_d of 0.012 A/cm^2 and a peak D^* of 2.3 × 10^9 cm·Hz$^{1/2}$/W. The quantum efficiency is low in this proof-of-concept device, but it can be improved using a thicker N-MWSL absorber combined with a lower doping level. These results suggest that the PNn design grown by MOCVD is a promising option for a HOT MWIR photodetector.

Acknowledgements

The authors are grateful for the ShanghaiTech University Quantum Device Lab. This project is supported partly by the Natural Science Foundation of China with Grant No. 61874179, No. 61804161, No. 61975121 and No. 61605236, and partly by the National Key Research and Development Program of China (No. 2019YFB2203400).

References

[1] Martyniuk P, Rogalski A. HOT infrared photodetectors. Opto Electron Rev, 2013, 21, 239

[2] Markovitz T, Pivnik I, Calahorra Z, et al. Digital 640x512/15μm InSb detector for high frame rate, high sensitivity, and low power applications. Infrared Technology and Applications XXXVII, 2011, 8012, 80122Y

[3] Klipstein P, Aronov D, Ezra M B, et al. Recent progress in InSb based quantum detectors in Israel. Infrared Phys Technol, 2013, 59, 172

[4] Jóźwikowski K, Kopytko M, Piotrowski J, et al. Near-room temperature MWIR HgCdTe photodiodes limited by vacancies and dislocations related to Shockley-Read-Hall centres. Solid State Electron, 2011, 63, 8

[5] Smith D L, Mailhiot C. Proposal for strained type II superlattice infrared detectors. J Appl Phys, 1987, 62, 2545

[6] Grein C H, Young P M, Flatté M E, et al. Long wavelength InAs/InGaSb infrared detectors: Optimization of carrier lifetimes. J Appl Phys, 1995, 78, 7143

[7] Nguyen B M, Chen G X, Hoang M A, et al. Growth and characterization of long-wavelength infrared type-II superlattice photodiodes on a 3-in GaSb wafer. IEEE J Quantum Electron, 2011, 47, 686

[8] Razeghi M, Abdollahi Pour S, Huang E K, et al. Type-II InAs/GaSb photodiodes and focal plane arrays aimed at high operating temperatures. Opto Electron Rev, 2011, 19, 261

[9] Höglund L, Asplund C, Marcks von Würtemberg R, et al. Manufacturability of type-II InAs/GaSb superlattice detectors for infrared imaging. Infrared Phys Technol, 2017, 84, 28

[10] Sun Y Y, Wang G W, Han X, et al. 320 × 256 high operating temperature mid-infrared focal plane arrays based on type-II InAs/GaSb superlattice. Superlattices Microstruct, 2017, 111, 783

[11] Gautam N, Myers S, Barve A V, et al. Band engineered HOT mid-wave infrared detectors based on type-II InAs/GaSb strained layer superlattices. Infrared Phys Technol, 2013, 59, 72
[12] Teng Y, Zhao Y, Wu Q H, et al. High-performance long-wavelength InAs/GaSb superlattice detectors grown by MOCVD. IEEE Photonics Technol Lett, 2019, 31, 185
[13] Zhao Y, Teng Y, Hao X J, et al. Optimization of long-wavelength InAs/GaSb superlattice photodiodes with Al-free barriers. IEEE Photonics Technol Lett, 2020, 32, 19
[14] Ting D Z Y, Soibel A, Höglund L, et al. Type-II superlattice infrared detectors. In: Advances in Infrared Photodetectors. Amsterdam: Elsevier, 2011
[15] Li X, Zhao Y, Wu Q H, et al. Exploring the optimum growth conditions for InAs/GaSb and GaAs/GaSb superlattices on InAs substrates by metalorganic chemical vapor deposition. J Cryst Growth, 2018, 502, 71
[16] Soibel A, Keo S A, Fisher A, et al. High operating temperature nBn detector with monolithically integrated microlens. Appl Phys Lett, 2018, 112, 041105
[17] Ting D Z Y, Hill C J, Soibel A, et al. A high-performance long wavelength superlattice complementary barrier infrared detector. Appl Phys Lett, 2009, 95, 023508

Xiujun Hao was born in Hebei, China. He received a BS degree from Suzhou University of Science and Technology in 2014. He is currently studying as a doctoral student in School of Physical Science and Technology, ShanghaiTech University, China. His major is Materials Science and Engineering and research interests are devices and nanostructures based on III–V compound semiconductors.

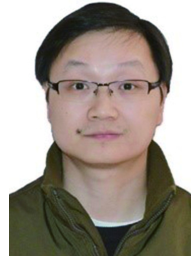

Yong Huang was born in Chongqing, China. He received a BS degree in Materials Science and Engineering from Tsinghua University in 2002 and a MS degree in Electronics and Optoelectronics from the Institute of Semiconductors, Chinese Academy of Sciences, in 2005 in Beijing, China. He earned a PhD degree in Electrical and Computer Engineering at Georgia Institute of Technology at Atlanta in 2010. He worked at IQE Inc. as a Senior Process Engineer from 2011 to 2014 at Taunton MA. He is currently a Professor at Suzhou Institute of Nano-Tech and Nano-Bionics, Chinese Academy of Sciences. His research interests are photonic and electronic materials, devices, and nanostructures based on III-V compound semiconductors.